Middle-East Journal of Scientific Research 24 (7): 2404-2417, 2016
ISSN 1990-9233

DOI: 10.5829/idosi.mejsr.2016.24.07.23722

A New Content-Based Image Retrieval Framework for Medical Applications

[1]Ananthi Sheshasaayee and [2]C. Jasmine

[1]Professor & Head, PG & Research Department of Computer Science,
Quaid-E-Millath Government College for Women, Chennai, Tamil Nadu, India
[2]Research Scholar, University of Madras, PG & Research Department of Computer Science,
Quaid-E-Millath Government College for Women, Chennai, Tamil Nadu, India

Abstract: In this paper, an approach for Content Based Image Retrieval (CBIR) in Medical Applications (IRMA) with particular focus on its Semantic gap measurement of classification modelling, its concept for feature representation, feature selection and distance computation for efficient implementation is presented. In addition, the proposed model is presented to some applications such as skull, hand and mammogram images of breast to show the general applicability of the concept. The method described in this work contains two major stages image analysis and image retrieval. The objective of the image analysis stage is to perform pre-processing stage using Median Filtering (MF) to remove noises from images samples, examine the global and local feature descriptors as well as textural features of mammograms and then test the statistical significance of the differences between normal and abnormal mammograms. In medical images texture feature plays a major role, so in this work texture features are extracted using Gray level Co-Occurrence Matrix (GLCM). These discriminating features are selected using Harmony Search (HS) to construct a feature descriptor of mammograms, skull and hand images. The descriptor constructed in the image analysis stage is embedded into the CBIR system. The feature descriptor is extracted from the query image in order to retrieve the mammograms, skull and hand images relevant to the query image. The Discriminative Dictionary Learning (DDL) is used in the proposed system to perform a similarity measure in the classified and indexed feature vector space. Hybrid Fuzzy Neural Network (HFNN) based Relevance Score (RS) mechanism is also adopted to reduce the semantic gap. Precision, Recall, F-measure, Accuracy, Sensitivity and Specificity metrics is used as a measure of performance in the proposed GLCM-HS-DDL system. The Experimental results reveal that the retrieval performance of the proposed GLCM-HS- DDL system for heterogeneous medical image database is better than the existing systems at high accuracy and less error rate.

Key words: Content Based Image Retrieval (CBIR) · In Medical Applications (IRMA) · Texture Feature Extraction · Gray Level Co-Occurrence Matrix (GLCM) · Relevance Feedback (RF) · Feature Selection and Harmony Search (HS)

INTRODUCTION

Medical images play a vital role in disease analysis, education, research, etc. Evolution of computer vision and digital imaging modalities has generated a vast amount of digital images in the medical domain. Consequently, the task of retrieving heterogeneous medical images from a large-scale image database becomes more difficult than ever before for a computer vision system due to the noise, variation in size, shape, color, illumination, etc. Hence, it is necessary to build up an appropriate system for medical image retrieval with efficient storage and effective retrieval to assist the physicians. The huge volume of medical images generated in hospitals creates a need to develop new tools to retrieve such visual information. The task of Content-Based Image Retrieval (CBIR) in the medical field is to help radiologists to retrieve images with similar contents. However, CBIR methods are usually developed for specific features of images, so that methods are not always applicable between different kinds of medical images.

Corresponding Author: Ananthi Sheshasaayee, Professor & Head, PG & Research Department of Computer Science, Quaid-E-Millath Government College for Women, Chennai, Tamil Nadu, India.

The conventional text-based image retrieval systems use textual keywords that are manually annotated on images. With the vast and diversity of images, textual keywords hold the disadvantages of laborious, tedious and time-consuming. Moreover, the manual annotation of the images strongly depends on what the users focus on and it may vary between persons and also vary in time for the same person. Thus, textual keywords are inefficient in providing sufficient and distinctive discriminatory power of the images. The picture archival and communication system (PACS) [1] compliant with digital imaging and communications in medicine (DICOM) format is used by most hospitals to handle huge collections of medical images. The PACS uses textual information stored in the DICOM header such as patient identity, date, type of examinations, modality, body parts examined, etc. for the image retrieval operations.

The literature reveals [1] that the DICOM headers include a high rate of errors and storing the DICOM format images in any of the compressed formats such as JPEG, TIFF, etc. leads to loss of DICOM header information. In order to improve the performance of PACS, content based image retrieval (CBIR) techniques have been proposed by several researchers in the PACS environment [1].Consequently, a number of researches have been focused on Content Based Medical Image Retrieval (CBMIR) to facilitate the physicians such as CBMIR system for High Resolution Computed Tomography (HRCT) images of the lung [2], PET images of the human brain [3], X-ray images of the human cervical and lumbar spines [4], Computed Tomography (CT) images of chest [5], a PathMiner system for pathological images [6], X-ray images of spine [7] , X-ray images of chest [8], mammogram images of breast [9] etc. However, the aforesaid literature is distinct to modalities, biological system, body orientation etc.

In recent reports, some approaches for content-based retrieval specially designed to support medical tasks have been published. Koran et al. describe a system for fast and effective retrieval of tumour shapes in mammogram x-rays [10]. This approach has certain restrictions on both the images (mammography only) and the features (tumour shapes only), which are supported by the system. Likewise, the Automatic Search and Selection Engine with Retrieval Tools (ASSERT) operates only on high-resolution computed tomography of the lung [11]. A physician delineates the region bearing pathology and marks a set of anatomical landmarks when the image is entered into the database. Hence, ASSERT has extremely high data entry costs, which prohibit its application for clinical routine.

Long *et al*. access a large collection of 17, 000 spine radiographs by means of shape analysis, where biomedical categories such as "anterior osteophytes present/not present" are distinguished automatically [12]. The data entry costs are low, but queries are limited to the pre-defined categories. Brain lesions are extracted automatically within three-dimensional data sets from computed tomography and magnetic resonance imaging. Their representation model consists of an additional knowledge- based layer within the semantic model. This layer provides a mechanism for accessing and processing spatial, evolutionary and temporal queries. Nonetheless, those concepts for medical image retrieval are task- specific, i.e. limited to a particular modality, organ, or diagnostic study and, hence, usually not directly transferable to other medical applications. However, the distinctive characteristics of descriptive text versus self-contained image information in general are well understood and, in particular, their impact on medical image databases intended to support indexing and retrieval is commonly appreciated.

Subsequently, described a heterogeneous medical image retrieval framework [13], which performs phase congruency process in L*a*b* colour space to extract edge co-operative maps and is processed using the SIFT to drive key points. The extracted key points are quantized to build a codebook using Spherical Self-Organizing Map (SOM) built with a geodesic data structure. Although many research works have been contributed to CBMIR, the retrieval accuracy of the existing CBMIR systems for heterogeneous medical image database is still limited and unsatisfactory due to the lack of techniques used to extract the efficient and effective features of the medical images. Though the system presented by Rahman *et al.* [14] has shown significantly better results when compared to the systems previously reported in the literature, the high dimensionality of the feature vector results in high computational and storage cost. Correspondingly, even if the system reported in [13] uses low feature vector dimension than the system of Rahman *et al.* [14], it results in less retrieval accuracy and the feature vector dimension is also not significantly less.

The main objective of the proposed system is to develop a more accurate and cost effective systems for supporting physicians. This paper, presents an approach for Content Based Image Retrieval in Medical Applications (IRMA) with particular focus on its Semantic gap measurement of classification modelling, its concept for feature representation, feature selection and distance computation for efficient implementation. In addition, proposed model is presented to some applications such

as skull, hand and mammogram images to show the general applicability of the concept. The method described in this work contains two major stages image analysis and image retrieval which is discussed detail in section 3. The image analysis performs the image pre-processing including the removal of noisy objects from the images.

Thus, the proposed system six types of features are extracted from feature extraction. In the first type of feature, color histogram is extracted to represent color and color moments such as mean, variance and skewness. In the second type of feature, Gabor Wavelet Transform (GWT) feature is also extracted for multichannel, multi-resolution analysis that represents image variations at different scales. In third type of feature Moving Picture Experts Group (MPEG)-7, there is a descriptor for edge distribution in the image. In fourth type Gradient Information with Scale and Temporal (GIST) descriptor is proposed to develop a low dimensional representation of the scene, which does not require any form of segmentation. In fifth type , Local Binary Pattern (LBP) analysis the texture parameters of images might reveal more important information In the LBP method, the eight neighbour pixels for each pixel in the ROI were examined and an 8-bit LBP-value was calculated. In final feature Texture feature extraction is done using Gray Level Co- occurrence Matrix (GLCM). For extracted features dimensionality reduction or feature selection is performed using Harmony Search (HS). Feature selection removed the features of low discriminant power and reduces space dimensions. Hybrid Fuzzy Neural Network (HFNN) based Relevance Score (RS) is using positive and negative examples provided by the user to improve the system's performance [15].

Proposed Methodology: In this paper, present an approach for Content Based Image Retrieval in Medical Applications (IRMA) with particular focus on its Semantic gap measurement of classification modelling, its concept for feature representation, feature selection and distance computation for efficient implementation. In addition, proposed model is presented to some applications such as skull, hand and mammogram images to show the general applicability of the concept. The method described in this work contains two major stages image analysis and image retrieval. The objective of the image analysis stage is to perform pre-processing stage to remove noises from images samples, examine the global and local feature descriptors as well as textural features of mammograms and then test the statistical significance of the differences between normal and abnormal mammograms. These discriminating features are selected to construct a feature descriptor of mammograms, skull and hand images. The descriptor constructed in the image analysis stage is embedded into the CBIR system. The feature descriptor is extracted from the query image in order to retrieve the mammograms, skull and hand images relevant to the query image. The performance of the CBIR system is then evaluated. The detailed steps and components of the experiment are described in the following sections.

Pre-Processing Using Median Filtering: The image analysis performs the image pre-processing including the removal of noisy objects from the images. Pre-processing is the name used for operations on images at the lowest level of abstraction. The aim of the pre-processing is an improvement of the image that suppresses unwilling distortions or enhances some image features, which is important for future processing of the images. This step focuses on image feature processing. The median filter is a nonlinear signal processing technology based on statistics [15]. The noisy value of the digital image or the sequence is replaced by the median value of the neighbourhood (mask). The pixels of the mask are ranked in the order of their gray levels and the median value of the group is stored to replace the noisy value. The median filtering output is $g(x, y) = \text{med}\{f(x - I, y - j), i, j, \in W\}$, where f(x, y(, g(x, y) are the original image and the output image respectively, W is the two-dimensional mask: the mask size is n × n (where n is commonly odd) such as 3 × 3, 5 × 5 and etc.; the mask shape may be linear, square, circular, cross and etc. The noise-reducing performance of the median filter: Because the median filter is a nonlinear filter, its mathematical analysis is relatively complex for the image with random noise. For an image with zero mean noise under normal distribution, the noise variance of the median filtering is approximately.

$$\sigma_{med}^2 - \frac{1}{4nf^2(\bar{n})} \approx \frac{\sigma_i^2}{n + \frac{\pi}{2} - 1}, \frac{\pi}{2} \quad (1)$$

where σ_i^2 is input noise power (the variance), n is the size of the median filtering mask, $f(\bar{n})$ (is the function of the noise density. And the noise variance of the average filtering is;

$$\sigma_0^2 = \frac{1}{n}\sigma_i^2 \quad (2)$$

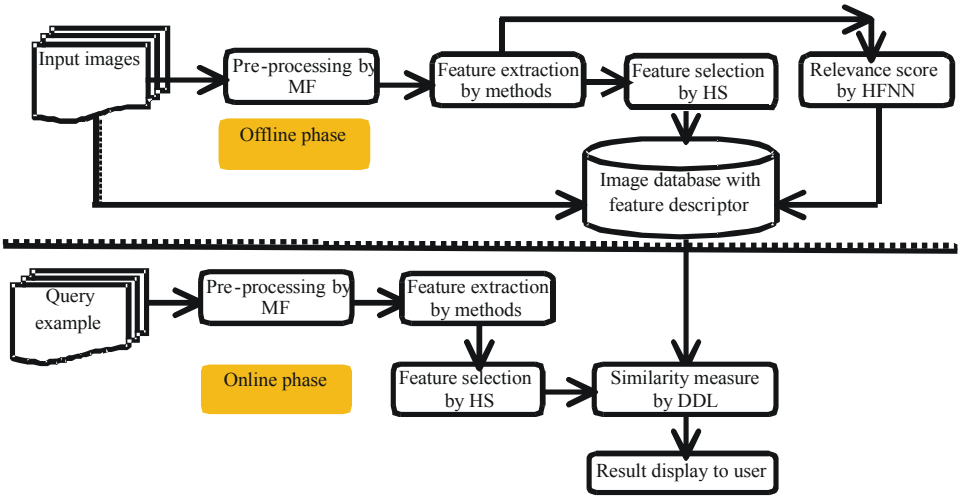

Fig. 1: Methodology of Content-Based Image Retrieval for Medical Applications (IRMA)

Comparing of (1) and (2), the median filtering effects depend on two things: the size of the mask and the distribution of the noise. The median filtering performance of random noise reduction is better than the average filtering performance, but to the impulse noise, especially narrow pulses are farther apart and the pulse width is less than n/2, the median filter is very effective. The median filtering performance should be improved if the median filtering algorithm, combined with the average filtering algorithm, can adaptively resize the mask according to the noise density. A pre-processing step has been introduced to remove background noise and to enhance structural features.

Feature Extraction: The methodology for the CBIR is based on comparing image content from a noise removed images to earlier cases. All clinically used methods refer to the epiphysis area between the samples, so the extraction of the features from the noise removed images becomes very important. Therefore extract those areas as epiphyseal Regions of Interest (eROIS) of each image in a standardized way. Instead of applying a query on the complete image, every eROI is used for an individual query to the database. The feature extraction step derives local image descriptions, i.e. a feature value (or a set of values) is obtained for each pixel. Then most significant six categories of features are extracted in this phase.

Color Histogram and Color Moments (81 Dimensions): In color histograms, quantization is a process where number of bins is reduced by taking colors that are similar to each other and placing them in the same bin. Quantizing reduces the space required to store the histogram information and time to compare the histograms. Obviously, quantization reduces the information regarding the content of images; this is the tradeoffs between space, processing time and accuracy in results [16].

Colour moments [17] as feature vectors for image retrieval. Since any color distribution can be characterized by its moments and most information is concentrated on the low-order moments, only the first moment (mean), the second moment (variance) and the third moment (skewness) are taken as the feature vectors. The similarity between two colour moments is measured by the Euclidean distance. Two similar images will have high similarity. However, if two images have only a similar sub-region, their corresponding moments will be different and the similarity measure will be low.

Gabor Wavelets Transform(120 Dimensions): Gabor Wavelet Transform (GWT) is a classic method for multichannel, multi-resolution analysis that represents image variations at different scales. Gabor filters are a group of wavelets obtained from the appropriate dilation and rotation of Gabor function: a Gaussian modulated sinusoid. By capturing image details at specific scales and specific orientations, Gabor filters present a good similarity with the receptive fields on the cells in the primary visual cortex of the human brain. Gabor wavelet transform provides a flexible method for designing efficient algorithms to capture more orientation and scale information [18]. As each Gabor filter or wavelet captures a specific frequency and a specific direction from the image, texture feature extraction using this representation requires the re-convolution of the image with the Gabor function for each change of one of these parameters.

Edge Direction Histogram (37 Dimensions): In Moving Picture Experts Group (MPEG)-7, there is a descriptor for edge distribution in the image. This edge histogram descriptor proposed for MPEG-7 [19] consists only of local edge distribution in the image. That is, since it is important to keep the size of the histogram as small as possible for the efficient storage of the metadata, the normative edge histogram for MPEG-7 is designed to contain only local edge distribution with 80 bins. These 80 histogram bins are the only standardized semantics for the MPEG-7 edge histogram descriptor. However, with the local histogram bins only, it is not sufficient to represent global features of the edge distribution. Note that to improve the retrieval performance, need global edge distribution as well.

GIST Features (512 Dimensions): The Gradient Information with Scale and Temporal (GIST) descriptor [20]. The idea is to develop a low dimensional representation of the scene, which does not require any form of segmentation. The authors propose a set of perceptual dimensions (naturalness, openness, roughness, expansion, ruggedness) that represent the dominant spatial structure of a scene. They show that these dimensions may be reliably estimated using spectral and coarsely localized information. The image is divided into a 4-by-4 grid for which orientation histograms are extracted. The GIST descriptor has recently shown good results for image search.

Binary Pattern

Local Binary Pattern (59 Dimensions): Local Binary Pattern (LBP) analysis the texture parameters of images might reveal more important information In the LBP method, the eight neighbor pixels for each pixel in the ROI were examined and an 8-bit LBP-value was calculated. Weight positions in the LBP weight matrix were set to be perpendicular to fibers to get better enhancement of the fibers. LBP is built by thresholding neighbor pixels by the grayscale value of the center pixel and multiplying the binary matrix with the weight matrix. Weights were set to be perpendicular to bone fibers to get better enhancement of the fibers.

Adaptive Local Binary Pattern (72 dimensions) (ALBP): In [21] used the oriented standard deviation information of the neighborhood in the matching step to obtain rotation invariance. ALBP method which considers different sizes of the neighborhood in order to create a unique feature vector for rotation invariance. To this end, an Adaptive LBP (ALBP) scheme is proposed here to minimize the difference along different orientation of texture features. Specifically, this work introduces a parameter we_p so that the overall difference $|g_c - we_p * g_p|$ can be minimized. The objective function is as follows:

$$we_p = \arg\min_{we}\{\sum_{i=1}^{N}\sum_{j=1}^{M}| g_c(i,j) - we * g_p(i,j) |^2\} \quad (3)$$

The Least Square Estimation (LSE) technique can be used for such an optimization and the weight we_p can be easily computed as follows:

$$we_p = \frac{\vec{g}_p^{T}\vec{g}_c}{\vec{g}_p^{T}\vec{g}_p} \quad (4)$$

where $\vec{g_c} = [g_c(1,1), g_c(1,2);...; g_c(N,M)]$ is a column vector containing all the possible $g_c(i,j)$ image pixels and $\vec{g_p} = [g_p(1,1), g_p(1,2);...; g_p(N,M)]$ is the corresponding vector for all $g_p(i,j)$ image pixels. Each weight we_p is estimated along one orientation $2\pi p/P$ for the whole image. Finally, the ALBP is defined as:

$$ALBP_{p,R} = \sum_{p=0}^{P-1} s(g_p * we_p * g_c)2^P \quad (5)$$

where P the total number of involved neighbours and R is the radius of the neighbourhood pixels of images. Let $\vec{we} = [we_0, we_2, ..., we_{p-1}]$ be the ALBP weight vector. ALBP weight vector is also shifted with the rotation of the image and it can align $\vec{we}$ of two different BAA image samples.

Texture Feature Extraction Using Gray Level Co-Occurrence Matrix (GLCM): Gray Level Co- occurrence Matrix (GLCM) is a matrix that depicts the number of occurrences of one gray level for fake and live fingerprint image making appearance in a given spatial linear relationship with another gray level within the area of detection.GLCM calculates second order texture features, which in turn, are of greatersignificance in human vision and realizes a similar level of categorization performance. This mechanism is normally employed in texture analysis as it is capable for providing for each sample a huge collection of fake and live fingerprint image features and it can be assumed that at least any one of these features are able to present even a smaller variation of texture between multiple classes.GLCM of an $N_x \times N_y$ image, which comprises of pixels with gray levels $(0,1,....,G-1)$ is a two dimensional matrix P(i,j) where each element of the matrix shows the probability of joint occasion of intensity levels k and l at a particular distance d. GLCM features selected are as shown below:

Contrast (CON): Contrast is the main diagonal close to the moment of inertia, which specifies how the values of the matrix are allocated and number of images of local transformations which is the reflection of the image clarity and texture of shadow depth. Larger Contrast means deeper texture.

$$CON = \sum_{n=0}^{N_g-1} n^2 \left\{ \sum_{i=1,|i-j=n}^{N_g} \sum_{j=1}^{N_g} p(i,j) \right\} \tag{6}$$

Correlation (CORR): Correlation is defined as a measure of gray level linear dependency of the pixels at the particular locations which are relative to each other.

$$CORR - \frac{\left[\sum_{i=1}^{N_g} \sum_{j=1}^{N_g} (i,j) p(i,j) - \mu_x \mu_y \right]}{\sigma_x \sigma_y} \tag{7}$$

$$\mu_x = \sum_{i=1}^{N_g} \left[i \sum_{j=1}^{N_g} p(i,j) \right] \tag{8}$$

$$\mu_y = \sum_{j=1}^{N_g} \left[j \sum_{i=1}^{N_g} p(i,j) \right] \tag{9}$$

$$\sigma_x = \sum_{i=1}^{N_g} \left[(i-\mu_x)^2 j \sum_{j=1}^{Ng} p(i,j) \right] \tag{10}$$

$$\sigma_y = \sum_{i=1}^{N_g} \left[(j-\mu_x)^2 i \sum_{i=1}^{Ng} p(i,j) \right] \tag{11}$$

where μ_x, μ_y are the mean values and σ_x, σ_y are the standard deviations of P_x and P_y, respectively.

Energy (ENER): This value is also referred to as Uniformity or Angular second moment. It figures the textural consistency which is pixel pair repetitions. It performs the identification of this array in textures. The maximum value of energy reaches to one. High energy values occur when gray level distribution is uniform or in a periodic form. Energy has a normalized range. The GLCM of less uniform image will have a large number of smaller entries.

$$ENER = \sum_{i=1}^{N_g} \sum_{j=1}^{N_g} P(i,j)^2 \tag{12}$$

Entropy (ENT): It is quite tricky to define the term Entropy. The concept comes from thermo dynamics, which refers to the quantity of energy that is lost in a persistent manner to heat each time a reaction or a physical transformation takes place. Entropy cannot be rejuvenated to do useful work. As a result of this, the term can be taken as q quantity of irrecoverable chaos or disorder.

$$ENT = \sum_{i=1}^{N_g} \sum_{j=1}^{N_g} [P(i,j) log(P(i,j))] \tag{13}$$

Inverse Difference Moment (IDM): IDM is generally called homogeneity that calculates the local uniformity of an image. IDM feature learns the measures of the proximity of the distribution of the GLCM elements with respect to the GLCM diagonal. IDM weight value is the reverse of the contrast weight, with an exponential decline in weights away from the diagonal.

$$IDM = \sum_{i=1}^{N_g} \sum_{j=1}^{N_g} \left[\frac{1}{1+(i-j)^2} P(i,j) \right] \tag{14}$$

Sum of Squares (SOS): The estimated variance of the source population is denoted by the sum of squared deviates of the images.

$$SOS = \sum_{i=1}^{N_g} \sum_{j=1}^{N_g} (i-\mu)^2 p(i,j) \tag{15}$$

Sum Average (SA): Sum average is the average of normalized gray tone image in the respective spatial domains.

$$SA = \sum_{i=2}^{2N_g} [i P_{x+y}(i)] \tag{16}$$

Sum Variance (SV): This characteristic applies relatively high weight age on the elements that vary from the average value of $P(i,j)$.

$$SV = \sum_{i=2}^{2N_g} [(i-SA)^2 P_{x+y}(i)] \tag{17}$$

Sum Entropy (SE): The sum entropy is a quantity of stochasticity within an image and it is given as,

$$SE = \sum_{i=2}^{2N_g} [P_{x+y}(i) log[P_{x+y}(i)]] \tag{18}$$

Difference Variance (DV): The difference variance is the variation of the image in a normalized co-occurrence matrix.

$$DV = -\sum_{i=0}^{N_g-1}[(i-f']P_{x-y}(i)] \text{ where } f' = \sum_{i=0}^{N_g-1}\left[iP_{x-y}(i)\right] \quad (19)$$

Difference Entropy (DE): The difference entropy is also an *amount of an image randomness indicator.

$$DE = -\sum_{i=0}^{N_g-1}[P_{x-y}(i)]\log[P_{x-y}(i)]] \quad (20)$$

Area (A): The area A_i is calculated in pixels and is an indication of the relative size of the object.

$$A_i = \Sigma\Sigma I_i(r,c),\ 0 \le r, \le N-1 \quad (21)$$

where:

$$I_i(r,c) = \begin{cases} 1 \text{ if } I(r,c) \text{is } i^{th} \text{ object} \\ 0 \text{ otherwise} \end{cases} \quad (22)$$

Perimeter (P): The perimeter is a measure of the count of the number of '1' pixels that have '0' pixels as neighbours in the original binary image.

Mean (M): Standard deviation or variance represents the contrast of an image. Image with good contrast should have a big variance. Standard Deviations (SD) also depict the cluster.

$$mean: \mu = \sum_{i=1}^{L} k_i p(k_i) \quad (23)$$

Variance (V): Variance denotes the variations of an image.

$$variance: \sigma^2 = \sum_{i=1}^{L}(k_i-\mu)^2 p(k_i) \quad (24)$$

Skewness (SK): Skew is a measure of the non-uniformity (imbalance) of the distribution of the gray level.

$$skewnesss: \mu_3 = \sigma^{-3}\sum_{i=1}^{L}(k_i-\mu)^{-3} p(k_i) \quad (25)$$

Kurtosis (K): It denotes the level of sharpness which is relatively the curve of an image,

$$Kurtosis: \mu_4 = \sigma^{-4}\sum_{i=1}^{L}(k_i-\mu)^{-4} p(k_i) - 3 \quad (26)$$

Standard Deviation (SD)

$$standard\ deviation: \sqrt{variance} \quad (27)$$

where k_i = gray value of the i^{th} pixel, L = number of distinctive gray levels, $p(k_i)$ normalized texture feature gray level value.

$$p(k_i) = \frac{number\ of\ pixels\ with\ gray\ level\ of\ I}{total\ number\ of\ pixels\ in\ the\ region} \quad (28)$$

Gradient (G) is a vector which has certain magnitude and direction:

$$\nabla_f = \frac{\partial_f}{\partial_x}\hat{x} + \frac{\partial f}{\partial y}\hat{y} \quad (29)$$

where: $\frac{\partial_f}{\partial_x}$ is the gradient in the x direction, $\frac{\partial f}{\partial y}$ is the gradient in the y direction. The gradient direction can be calculated by the formula:

$$\theta = \text{atan}^2\left(\frac{\partial f}{\partial x}, \frac{\partial f}{\partial y}\right) \quad (30)$$

Eccentricity (Ecc): Eccentricity is defined as a scalar value which specifies the eccentricity of the ellipse and has the same second moments as the region. The eccentricity is the ratio of the distance between the foci of the ellipse and its major axis length. The range value of eccentricity is from 0 to 1.

Zero-crossing is a measurement of the number of edges in a given image and by perception may show how "busy" a given textured image is. The calculation of the zero-crossing values it is first necessary to threshold each of the high-pass variant wavelet decomposition outputs in order to obtain binary images. The threshold value for each of the wavelet decomposition outputs is chosen to be its mean.

Global Features: These global features have been extensively employed in the previous CBIR researches. In case of local features, obtain the bag-of-visual-words features by means of two categories of descriptors:

- SIFT descriptor adopt the Hessian-Affine interest area detector with threshold 500; and
- SURF descriptor implements the SURF detector with threshold 500.

In case of the clustering phase, implement a forest of 16 kd-trees and look for 2, 048 neighbours to accelerate the clustering process. In the end, implement the TF-IDF weighing scheme to produce the concluding bag of- visual-words representation. By means of

selecting different descriptors (SIFT/SURF) and vocabulary sizes (200/1, 000), completely extracted four kinds of local features: SIFT200, SIFT1000, SURF200 and SURF1000. So features extraction phase six different type of features are extracted.

Feature Selection Using Harmony Search: Decoupling feature selection from feature extraction allows the integration of both the image category and query context into the abstraction process. For instance, the same radiograph might be subject to fracture or cancer examination, resulting in a contour-based or texture-based combination of features, the so-called feature sets, such as the contour set or texture set, respectively. In order to avoid exhaustive computation during query processing, these feature sets are pre-computed for each image in each likely category. For extracted features dimensionality reduction or feature selection is performed using Harmony Search (HS). Feature selection removed the features of low discriminant power and reduces space dimensions. From the selected carpal bone parameters, the skeletal age could be estimated by further analysis. This system demonstrated the importance of using a multidimensional feature analysis. It also showed that area, perimeter, ratio, number of carpal bones local features and global features were the most important features to be considered. These parameters together with the parameters extracted from the phalangeal analysis could be used to assess the bone ages. Harmony Search (HS) [22] is an evolutionary algorithm inspired in the improvisation process of music players. Basically, any possible feature selection solution is modelled as a harmony and each feature of the images to be optimized can be seen as a musical note. The best harmony called solution is chosen as the one that maximizes some optimization criteria.The Harmony Search (HS) algorithm is an interesting approach for several applications mainly because of its simplicity and low computational cost. The working procedure of HS is extended from recent work [8].

Relevance Score Learned Using Hybrid Fuzzy Neural Network (HFNN): Hybrid Fuzzy Neural Network (HFNN) based Relevance Score (RS) is using positive and negative examples provided by the user to improve the system's performance. The main goal of relevance score learning is to select relevant and irrelevant medical images provided by the user to improve the performance in CBIR system. For a given query, the system first retrieves a list of reduced image features according to predefined similarity metrics, which are often defined as the distance between feature vectors of images. Then, the user selects a set of relevant and irrelevant images from the retrieved images and the system subsequently refines the query and retrieves a new list of images. The key issue is how to incorporate relevant and irrelevant image to refine the query and how to adjust the similarity measure according to the feedback. Here this proposed work uses a Hybrid Fuzzy Neural Network (HFNN) relevance score method. This HFNN is a modified version of Multilayer Feed Forward Neural Network (MFNN) with four different layers [23]. There are four layers in an HFNN. The first layer is equivalent to the fuzzification with 2N neurons. Membership functions and numbers of fuzzy variables for the inputs need be determined in this layer. The second one is similar to the fuzzy if and then rule base with N^2 neurons. The number of neurons in the second layer is set equal to the maximum number of necessary if-then rules for a given fuzzy inference system. The last two layers are functionally equivalent to defuzzification. The combination of layer 3 and 4 is simply a MFNN with N neurons and single neuron. In practical implementation, bias vector is usually added in the layer 3 and layer 4 so that the HFNN is able to approximate mappings which assign nonzero relevant score to zero input images. Novel neural network architecture such as HFNN has been proposed in this work for RS, which provides a predefined similarity measure for accurate.

Discriminative Dictionary Learning for Similarity Measurement: Finally, images from the CBIR medical database, whose features fulfil the closest match, are selected and corresponding similarity matching process done using Discriminative Dictionary Learning (DDL). Measuring the semantic gap allow us to develop retrieval systems that are able to shorten or bridge the gap. Liu *et al.* [24] introduced a method based on information theory to measure the semantic gap. They considered the mutual information between the information quality of images and the user-desired information quality of images as the measure of semantic gap, where the user-desired information computed by comparing the results of a retrieval system to the user's query; and the similarity was measured based on low-level features of images. In this section present the details of proposed DDL approach for semantic gap measurement between the user query image and database images. DDL is formulated which learns a flexible nonlinear proximity function in order to enhance visual similarity search in CBIR.

$$X^* = \underset{x}{\operatorname{argmin}} \sum_{i=1}^{N} (\| y_i - Ax_i \|_2^2 + \gamma \| x_i \|_1) \tag{31}$$

where γ constant indicates a sparsely constraint factor and the term $\|y_i - Ax_i\|_2^2$ indicates the reconstruction error for matching results. In order to get hold of discriminative feature vector x by means of the pairwise constrained dictionary A, the objective function for dictionary creation is given as follows:

$$< A^*, X^* >= \underset{A,X}{\operatorname{argmin}} \sum_{i=1}^{N} (\| y_i - Ax_i \|_2^2 + \gamma \| x_i \|_1) + \frac{\beta}{2} \sum_{i,j=1}^{N} \| x_i - x_j \|_2^2 M_{ij} \tag{32}$$

$$\underset{A,X}{\operatorname{argmin}} \sum_{i=1}^{N} (\| y_i - Ax_i \|_2^2 + \gamma \| x_i \|_1 + \beta (Tr\left(X^T XD\right) - Tr\left(X^T XM\right)) \tag{33}$$

where the constants γ and β manage the virtual contribution of the resultant terms. The first term $\|y_i - Ax_i\|_2^2$ indicates the reconstruction error term, which assesses the reconstruction error of the approximation. The second term $\|x_i\|_1$ indicates the regularization term. The last term, which is fresh and proposed at this point, indicates the discrimination term called 'pair- wise error feature vector' in accordance with the pairwise constraints which are encoded in matrix M. $D = \text{diag}\{d_1, \ldots, d_N\}$ indicates a diagonal matrix where diagonal elements are the summations of the row elements of M,

$$d_i = \sum_{j=1}^{N} M_{ij} . L = D - M \tag{34}$$

L is the Laplacian matrix. Matrix M has various forms in accordance with the setbacks being taken into account. As a result, provided the sets of 'similar feature vectors from RS learning' and 'diverse feature vectors from RS learning' pairs S and D, characterize matrix M to encode the (dis)similarity information as given below,

$$M_{ij} = \begin{cases} +1 \; if (y_i, y_j) \in S \\ -1 if (y_i, y_j) \in D \\ 0 \; else \end{cases} \tag{35}$$

The objective function for learning a pairwise constrained dictionary A for query and input image feature vectors from FNN with both reconstructive and discriminative power can be given as:

$$< A^*, X^*, W^* >= \underset{A,X,W}{\arg\min} \sum_{i=1}^{N} (\|y_i - Ax_i\|_2^2 + \gamma \|x_i\|_1) + \frac{\beta}{2} \sum_{i,j=1}^{N} \|x_i - x_j\|_2^2 M_{ij} \quad + \alpha \sum_{i,j=1}^{N} \|h_i - Wx_i\|_2^2 + \lambda \|W\|_2^2 \tag{36}$$

$\left\| h_j - Wx_i \right\|_2^2 + \lambda \left\| W \right\|_2^2, \left\| h_i - Wx_i \right\|_2^2$ indicates the classification query matching error, $\|W\|_2^2$ indicates the regularization penalty term, assists in learning an optimal linear predictive classifier $h_i = [0,0,..,1,..,0,0]^T$ is a label vector related to a feature vectors results from HFNN learning, where non-zero position represents the class label of y_i.

EXPERIMENTATION RESULTS

In order to implement the proposed GLCM-HS-DDL system, have collected medical images. The experimental medical image database Mammogram dataset is collected from http://breastscreening.cancer.gov/data/mammograph y_dataset/. The number of images in the Mammogram in experimental database are 1510, 592, 858, 580, 1708, 663 and 489 respectively. The great majority of the hand and skull images have dimensions between 512 × 350 and 512 × 512 pixels, while the others usually are between 512 × 150 and 512 × 350 pixels, roughly the images are in tiff and jpeg format and they vary in size. Some sample images from the experimental database are shown in Figure 2.

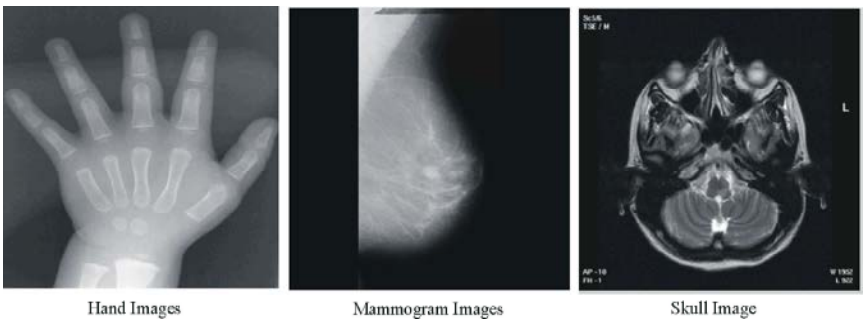

Fig. 2: Sample Query Images Taken from the Experimental Database

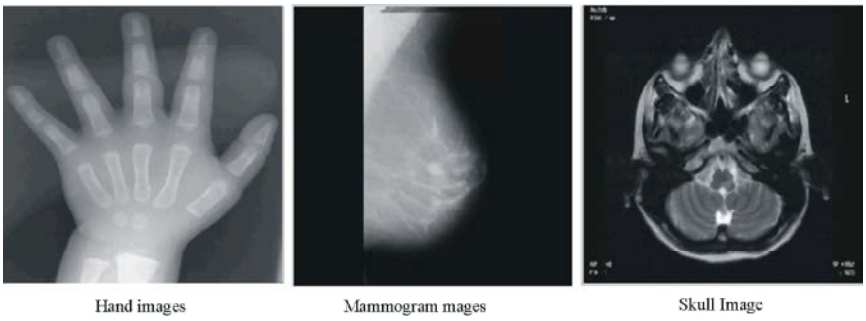

Fig. 3: Pre-processed Images

For query images pre-processed input image samples from the experimental database are shown in Figure. 3.

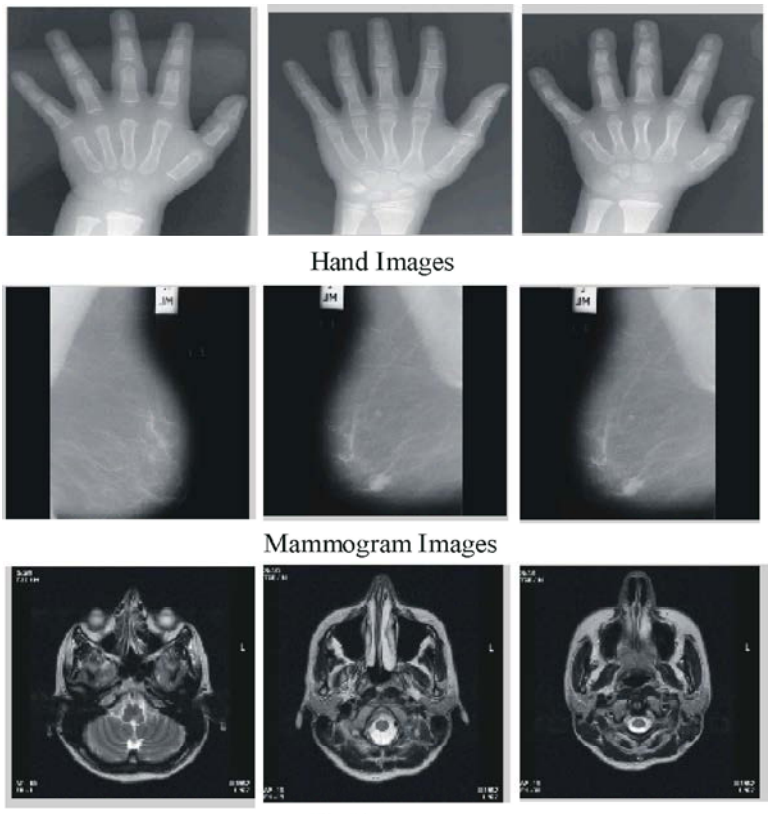

Fig. 4: Retrieved Images

For query images retrieved image samples from the experimental database are shown in Figure 4.

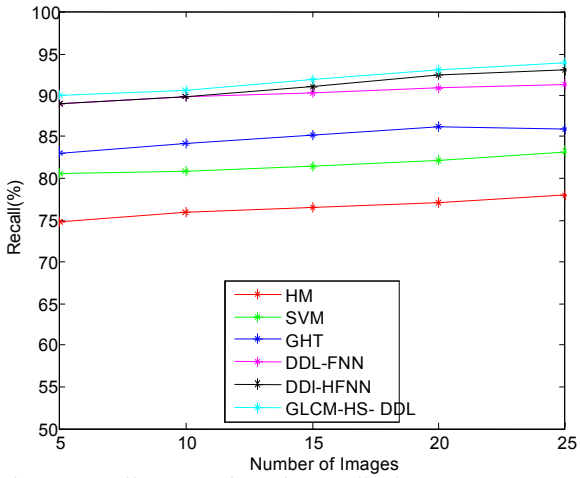

Fig. 5: Recall Comparison for Medical Images

In this work implemented the proposed GLCM-HS-DDL and conventional methods such as DDL-HFNN, DDL-FNN, GHT, SVM and HM for gray-scale medical images in experimental database. The retrieval performance of the proposed GLCM-HS-DDL is compared to that of conventional methods for the gray-scale medical images. It is observed from the results that the proposed GLCM-HS-DDL performs significantly better than that of the conventional methods for gray-scale medical images and the attained average retrieval rate of the proposed GLCM-HS-DDL and conventional methods for the gray-scale medical images are 93.8%, 93.12%, 91.63% , 86.98%, 84.21 % and 77.56% and respectively. The comparative results are shown in Figure.5 and it depicts the average recall of the proposed GLCM-HS-DDL and conventional methods for the medical images.

In this work implemented the proposed GLCM-HS-DDL and conventional methods such as DDL-HFNN, DDL-FNN, GHT, SVM and HM for gray-scale medical images in experimental database. It is observed from the results that the proposed GLCM-HS-DDL performs significantly better than that of the conventional methods for gray-scale medical images and the attained average precision rate of the proposed GLCM-HS-DDL and conventional methods for the gray-scale medical images are 79.83%, 77.58%, 76.83%, 72.58%, 62.63 % and 42.83% respectively. The comparative results are shown in Figure.6 and it depicts the average precision of the proposed GLCM-HS-DDL and conventional methods for the medical images.

From Figure 7 it is observed from the results that the proposed GLCM-HS-DDL performs significantly better than that of the conventional methods for gray-scale medical images and the attained average accuracy rate of the proposed GLCM-HS-DDL and conventional methods for the gray-scale medical images are 96.39%, 94.28%, 93.26%, 91.58%, 79.13 % and 71.68 % respectively. The comparative results are shown in Figure.7 and it depicts the average accuracy of the proposed GLCM-HS-DDL and conventional methods for the medical images.

From Figure 8 it is observed from the results that the proposed GLCM-HS-DDL performs significantly better than that of the conventional methods for gray-scale medical images and the attained average specificity rate of the proposed GLCM-HS-DDL and conventional methods for the gray-scale medical images are 95.83%, 94.52%, 93.56%, 78.59%, 70.83 % and 62.89 % respectively.

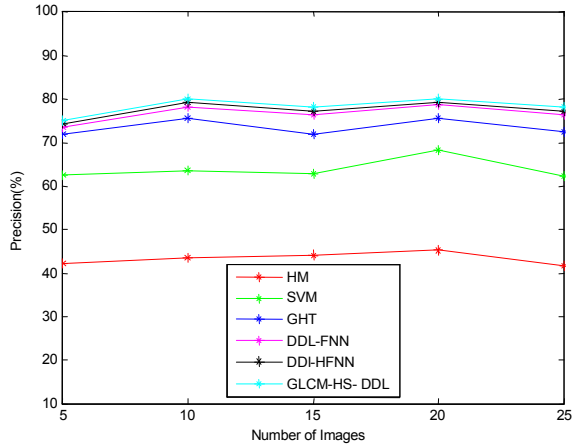

Fig. 6: Precision Comparison for Medical Images

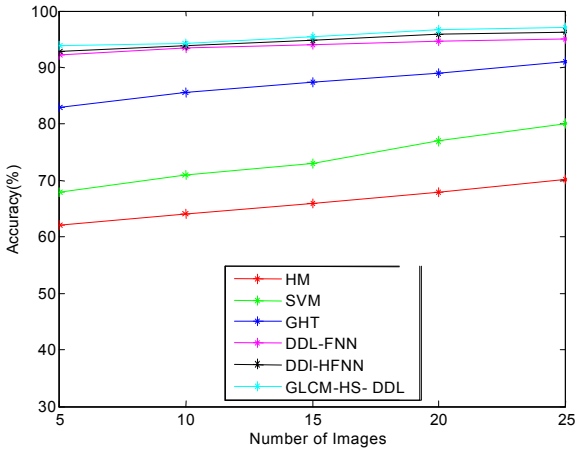

Fig. 7: Accuracy Comparison for Medical Images

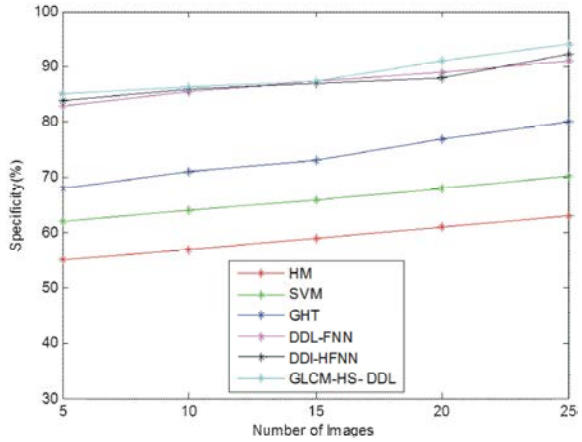

Fig. 8: Specificity Comparison for Medical images

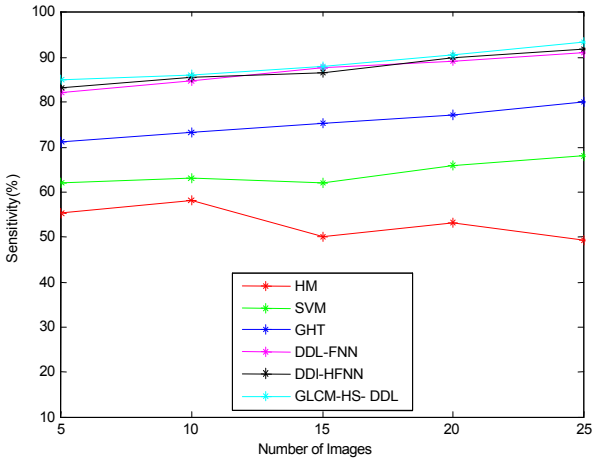

Fig. 9: Sensitivity Comparison for Medical Images

From Figure 9 it is observed from the results that the proposed GLCM-HS-DDL performs significantly better than that of the conventional methods for gray-scale medical images and the attained average sensitivity rate of the proposed GLCM-HS-DDL and conventional methods for the gray-scale medical images are 93.28 %, 91.86%, 90.88%, 79.58%, 70.83 % and 62.89 % respectively.

CONCLUSION

In contrast to specific applications, a general CBIR approach for medical images is presented and implemented combining a central database with distributed system architecture suitable for large image databases such as within a picture archiving and communication system. The IRMA system supports rapid prototyping and quick integration of novel image analysis methods. So far, the IRMA system is used to answer primitive queries on the image category level. This paper presents an approach for Content Based Image Retrieval in Medical Applications (IRMA) with particular focus on its Semantic gap measurement of classification modelling, its concept for feature representation, feature selection and distance computation for efficient implementation. In addition, proposed model is presented to some applications such as skull, hand and mammogram images to show the general applicability of the concept. The method described in this work contains two major stages image analysis and image retrieval. The objective of the image analysis stage is to perform pre-processing stage to remove noises from images samples, examine the global and local feature descriptors as well as textural features of mammograms and then test the statistical significance of the differences between normal and abnormal mammograms. These discriminating features are selected to construct a feature descriptor of mammograms, skull and hand images. The descriptor constructed in the image analysis stage is embedded into the CBIR system. The feature descriptor is extracted from the query image in order to retrieve the mammograms, skull and hand images relevant to the query image. The performance of the CBIR system is then evaluated. However, these experiments already have proven the validity and applicability of the IRMA concept. Resulting from system transparency, IRMA is suitable for sophisticated image processing to be performed by a medical user. In other words, CBIR principles are made available for a variety of medical applications. Hence, IRMA narrows the gap between the semantic imprint of an image and any alpha- numerical description that is always incomplete.Some of the major challenges in the area of medical image retrieval are outlined as follows:

- Extraction of robust and precise visual features from medical images is a difficult problem.
- The use of CBIR in medical diagnostics is important though it is difficult to realize.
- To be used as a diagnostic tool, the CBIR systems need to prove their performance to be accepted by the clinicians.
- In medical application domain many systems have been proposed where database consists of images of various anatomical regions with variety of image modalities. The standard databases are useful as a

benchmark to test various approaches in a general image retrieval framework; however these approaches are not useful for diagnostics support systems where high precision is required. Useful semantics for medical image retrieval needs to be established. Image localization can also be added in pre-processing part so that system will focus on the consistent particular region of interest only and give more refined results.

REFERENCE

1. Müller, H., N. Michoux, D. Bandon and A. Geissbuhler, 2004. A review of content-based image retrieval systems in medical applications—clinical benefits and future directions, International journal of medical informatics, 73: 1-23.
2. Dash, J.K., S. Mukhopadhyay and Khandelwal, 2012. Content-Based Image Retrieval System for Interstitial Lung Diseases, Indian Journal of Medical Informatics, 6(1): 1-2.
3. Batty, S., J. Clark, T. Fryer and X. Gao, 2008. Prototype system for semantic retrieval of neurological PET images, Medical Imaging and Informatics, Springer Berlin Heidelberg., pp: 179-188.
4. Xu, X., D.J. Lee, S. Antani and L.R. Long, 2008. A spine X-ray image retrieval system using partial shape matching, Information Technology in Biomedicine, IEEE Transactions on, 12(1): 100-108.
5. Yu, S.N. and C.T. Chiang, 2004. Similarity searching for chest CT images based on object features and spatial relation maps, Engineering in Medicine and Biology Society, IEMBS '04, 26th Annual International Conference of the IEEE, pp: 1-5.
6. Chen, W., P. Meer, B. Georgescu, W. He, L.A. Goodell and D.J. Foran, 2005. Image mining for investigative pathology using optimized feature extraction and data fusion, Computer methods and programs in biomedicine, 79(1): 59-72.
7. Hsu, W., S. Antani, L.R. Long, L. Neve and G.R. Lhoma, 2009. SPIRS: a Web-based image retrieval system for large biomedical databases, International journal of medical informatics, 78: 13-24.
8. Avni, U., H. Greenspan, E. Konen, M. Sharon and J. Goldberger, 2011. X-ray categorization and retrieval on the organ and pathology level, using patch-based visual words, Medical Imaging, IEEE Transactions on, 30(3): 733-746.
9. Wei, C.H., Y. Li and P.J. Huang, 2011. Mammogram retrieval through machine learning within BI-RADS standards, Journal of biomedical informatics, 44(4): 607-614.
10. Korn, P.F., N. Sidiropoulos, C. Faloutsos, E. Siegel and Z. Protopapas, 1998. Fast and effective retrieval of medical tumor shapes, IEEE Transactions on Knowledge and Data Engineering, 10(6): 889-904.
11. Shyu, C.R., C.E. Brodley, A.C. Kak, A. Kosaka, A.M. Aisen and L.S. Broderick, 1999. ASSERT: a physician-in-the-loop content-based retrieval system for HRCT image databases, Computer Vision and Image Understanding , 75(1): 111-132.
12. Long, L.R., S. Antani, D.J. Lee, D.M. Krainak and G.R. Thoma, 2003. Biomedical information from a national collection of spine x-rays: film to content-based retrieval, Medical Imaging, International Society for Optics and Photonics, pp: 70-84.
13. Sudhakar, M.S. and K. Bhoopathy Bagan, 2014. An effective biomedical image retrieval framework in a fuzzy feature space employing Phase Congruency and GeoSOM, Applied Soft Computing, 22: 492-503.
14. Rahman, M.M., D. You, M.S. Simpson, S.K. Antani, D. Demner-Fushman and G.R. Thoma, 2013. Multimodal biomedical image retrieval using hierarchical classification and modality fusion, International Journal of Multimedia Information Retrieval, 2(3): 159-173.
15. Zhu, Y. and C. Huang, 2012. An improved median filtering algorithm for image noise reduction, Physics Procedia, 25: 609-616.
16. Lew, M.S., N.Sebe, C. Djeraba and R. Jain, 2006. Content-based multimedia information retrieval: State of the art and challenges, ACM Transactions on Multimedia Computing, Communications and Applications (TOMM), 2.1: 1-19.
17. Stricker, M.A. and M. Orengo, 1995. Similarity of color images, IS&T/SPIE's Symposium on Electronic Imaging: Science & Technology. International Society for Optics and Photonics, pp: 381-392.
18. Jie, Y., Z. Qiang and Z. Liang, 2009. Research on texture images retrieval based on the Gabor wavelet transform, Information Engineering, ICIE'09. WASE International Conference on, IEEE, 1: 79-82.
19. Park, S.J., D.K. Park and C.S. Won, 2000. Core Experiments on MPEG-7 Edge Histogram Descriptor ISO, 5984.

20. Oliva, A. and A. Torralba, 2001. Modeling the shape of the scene: A holistic representation of the spatial envelope, International journal of computer vision, 42(3): 145-175.
21. Guo, Z., L. Zhang, D. Zhang and S. Zhang, 2010. Rotation invariant texture classification using adaptive LBP with directional statistical features, 2010 17th IEEE International Conference on Image Processing (ICIP), pp: 285-28.
22. Mashinchi, M.H., M.A. Orgun, M. Mashinchi and W. Pedrycz, 2011. A tabu–harmony search-based approach to fuzzy linear regression, IEEE Transactions on Fuzzy Systems, 19(3): 432-448.
23. Chuang, C.H. and T.S. Lee., 1996. A hybrid fuzzy neural network and its control applications, Proceedings of the 1996 IEEE International Symposium on Intelligent Control, pp: 175-180.
24. Liu, C. and G. Song, 2011. A method of measuring the semantic gap in image retrieval, using the information theory, 2011 International Conference in Image Analysis and Signal Processing (IASP), pp: 287-291.